Low Complexity Channel Estimation for 3GPP LTE Downlink MIMO OFDM Systems

Ömer Çetin*, Bahattin Karakaya* and Hakan Ali Çırpan‡
*Department of Electrical and Electronics Engineering,
İstanbul University, Avcılar Campus, 34320, İstanbul, Turkey
Email: omercetin@ieee.org, bahattin@istanbul.edu.tr
‡Department of Electronics and Communication Engineering,
İstanbul Technical University, İTÜ Maslak Campus, 34469, İstanbul, Turkey
Email: cirpanh@itu.edu.tr

Abstract—**Multiple Input Multiple Output - Orthogonal Frequency Division Multiplexing (MIMO-OFDM) is a promising technique for reaching high data rates targeted in the 3rd Generation Partnership Project - Long Term Evolution (3GPP-LTE). MIMO-OFDM channel estimation schemes play a very important role on achieving this aim. However, the complexity of the estimators increases exponentially due to the structure of the MIMO systems. This causes an increase in the computational burden of the transceivers. As a result, the complexity of the channel estimators is becoming an important issue in real world MIMO-OFDM applications. In this paper, the performance of the low complexity Minimum Mean Square Error (MMSE) channel estimator scheme based on Karhunen-Loéve (KL) series expansion coefficients for the 3GPP-LTE Downlink MIMO-OFDM systems is examined. System level simulations are accomplished to compare the performances of the estimators under the spatially correlated channel coefficient variations.**

Index Terms—**3GPP, LTE, MIMO, OFDM, MMSE, Karhunen-Loéve.**

I. Introduction

OFDM is a high performance candidate for wireless communication systems owing to its many advantages, especially its performance in frequency-selective fading channels. Besides that, MIMO transceiver architecture has potential to improve the system capacity. Hence in 3GPP-LTE, combined MIMO-OFDM structure is anticipated to meet the demands of rapidly increasing number of applications on wireless mobile networks. In MIMO-OFDM systems channel state information is essential for the detection and equalization. In [1], 3GPP-LTE physical channels are described in detailed and modulation types are standardized. Besides that spatial channel models for MIMO simulations are described elaborately in [2]. In the time domain pilot-aided channel estimation, unoccupied subcarriers namely "guard bands", adversely affect the performance of the estimator [3]. In order to reduce the complexity of the estimators, MMSE estimation of the KL series expansion coefficients is examined in [4]–[6]. In this paper, we compare the performances of the MMSE estimations of the KL series expansion coefficients of the 3GPP-LTE MIMO channel. In the simulations, the performances of the MMSE estimator of the KL expansion and LS estimator under the different channel correlations are compared. The notation used in this paper is as follows:

$\mathbf{A}^T$	Transpose of $\mathbf{A}$.
$\mathbf{A}^H$	Conjugate transpose of $\mathbf{A}$.
diag($\mathbf{a}$)	Diagonal matrix of $\mathbf{a}$.
$\mathbf{I}_N$	$N \times N$ identity matrix.
$\mathbf{0}_N$	$N \times 1$ column vector with all zeros.
$E[.]$	The expectation operator.
$\mathbb{R}^N$	N dimensional space with real numbers.
$\mathbb{C}^N$	N dimensional space with complex numbers.
$\otimes$	Kronecker product.

II. Signal Model

The block diagram of the simplified 3GPP-LTE, MIMO-OFDM transmitter system with N_T transmit antennas is depicted in Figure 1. M-QAM modulated serial data stream is grouped into N_d sized blocks.

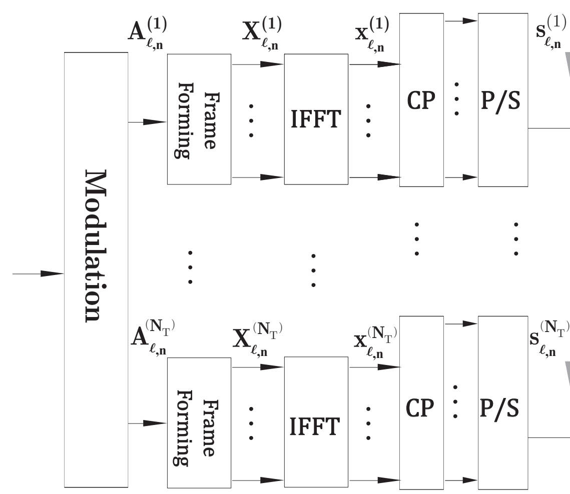

Fig. 1. MIMO-OFDM Transmitter scheme for LTE Downlink

A number of modulated N_{rs} reference signals, namely pilots and N_d sized data signals are allocated to the resource elements as defined in [1]. Reference and data signals have been paralleled into consecutive data blocks in order to constitute an OFDM symbol. At the pth transmit antenna, the ℓth OFDM symbol can be represented as

$$\mathbf{A}_\ell^{(p)} = [A_\ell^{(p)}[0], A_\ell^{(p)}[1], \ldots, A_\ell^{(p)}[N_{BW}-1]]^T \in \Xi^{N_{BW}} \quad (1)$$

where Ξ denotes the modulation alphabet and $N_{BW} = N_d + N_{rs}$ is the number of the occupied subcarriers at each of the transmit antenna. Before the N-point Inverse Fast Fourier Transform (IFFT) block, in order to avoid interference, N_{GB} zeros are

978-1-4244-9538-2/11/$26.00 © 2011 IEEE

padded to the unused subcarriers at the edges of the spectrum as guard bands, where N_{GB} is equal to $N - N_{BW}$. Only the specified OFDM symbols contain the reference signal for the channel estimation. Considering only the reference signal inserted OFDM symbols in the data-aided channel estimation, the OFDM symbol indicator ℓ could be omitted for the sake of simplicity. Reference and data signals with guard band before the IFFT block can be represented by $\mathbf{X}^{(p)} \in \Xi^N$ as below

$$\mathbf{X}^{(p)} = [0, \mathbf{A}_{left}^{(p)\ T}, \mathbf{0}_{N_{FFT}-N_{BW}}^T, \mathbf{A}_{right}^{(p)\ T}]^T \tag{2}$$

where

$$\begin{aligned} \mathbf{A}_{left}^{(p)\ T} &= [A^{(p)}[\frac{N_{BW}}{2}], \ldots, A^{(p)}[N_{BW}-1]]^T \\ \mathbf{A}_{right}^{(p)\ T} &= [A^{(p)}[0], A^{(p)}[1], \ldots, A^{(p)}[\frac{N_{BW}}{2}-1]]^T \ . \end{aligned} \tag{3}$$

N-point IFFT block is drived by the OFDM symbol $\mathbf{X}^{(p)}$ to generate time domain transmitted signal $\mathbf{x}^{(p)}$ is found to be

$$\mathbf{x}^{(p)} = \mathbf{F}\mathbf{X}^{(p)} \tag{4}$$

where

$$\mathbf{F} = \begin{bmatrix} 1 & 1 & \cdots & 1 \\ 1 & e^{j2\pi/N} & \cdots & e^{j2\pi(N-1)/N} \\ \vdots & \vdots & \ddots & \vdots \\ 1 & e^{j2\pi(N-1)/N} & \cdots & e^{j2\pi(N-1)(N-1)/N} \end{bmatrix} \tag{5}$$

is the DFT matrix. In order to get rid of the inter-symbol interference, Cyclic Prefix (CP) with a size of $N_{CP} \geq L$ is added to the signal $\mathbf{x}^{(p)}$ to obtain the time domain transmitted signal $\mathbf{s}^{(p)} \in \mathbb{C}^{N+N_{CP}}$. L represents the channel impulse response (CIR) vector length of the MIMO channel between the pth transmit antenna and the qth receive antenna where it can be expressed as $\mathbf{h}^{(qp)} = \left[h^{(qp)}[0], h^{(qp)}[1], \cdots, h^{(qp)}[L-1]\right] \in \mathbb{C}^{L}$. In Figure 2, MIMO-OFDM receiver scheme with N_R antennas is depicted. At each receive antenna, the signal $\mathbf{r}^{(q)} \in \mathbb{C}^{N+N_{CP}+L-1}$ can be expressed as the sum of the convolved signals $\mathbf{s}^{(p)}$ and $\mathbf{h}^{(qp)}$ from the transmit antennas. Before the FFT block at each receiver, unnecessary terms are removed and the signal combined into the subsequent blocks with a length of N termed as $\mathbf{y}^{(q)}$. In the light of above time domain expressions, the frequency domain representation of the received signal at the qth antenna $\mathbf{Y}^{(q)} = [Y^{(q)}[0], Y^{(q)}[1], ..., Y^{(q)}[N-1]]^T \in \mathbb{C}^{N}$ can be expressed as

$$\mathbf{Y}^{(q)} = \mathscr{X}\mathbf{H}^{(q)} + \mathbf{W}_n \tag{6}$$

where $\mathbf{W}_n \in \mathbb{C}^{N}$, is the additive white gaussian noise (AWGN) at the qth receive antenna with zero mean and covariance matrix $\mathbf{C}_{\mathbf{W}_n} = E[\mathbf{W}_n \mathbf{W}_n{}^H] = \sigma^2 \mathbf{I}_N$. $\mathscr{X}$ is the transmitted signal from all of the antennas in the frequency domain and can be represented as below

$$\mathscr{X} = [\mathbf{X}_{diag}^{(1)}, \mathbf{X}_{diag}^{(2)}, ..., \mathbf{X}_{diag}^{(N_T)}] \in \Xi^{N \times N_T N}, \tag{7}$$

where $\mathbf{X}_{diag}^{(p)} = diag\{\mathbf{X}^{(p)}\} \in \Xi^{N \times N}$ and $p \in 1, 2, ..., N_T$. $\mathbf{H}^{(q)} \in \mathbb{C}^{N_T N}$ is the combined channel frequency response (CFR) from all of the transmit antennas to the qth receive antenna, expressed by

$$\mathbf{H}^{(q)} = \left[\mathbf{H}^{(q1)T}, \mathbf{H}^{(q2)T}, ..., \mathbf{H}^{(qN_T)T}\right]^T \ . \tag{8}$$

$\mathbf{H}^{(qp)} \in \mathbb{C}^{N}$'s are the CFR between the pth transmit antenna and the qth receive antenna and can be obtained as below

$$\mathbf{H}^{(qp)} = \mathbf{F}_L \mathbf{h}^{(qp)}, \tag{9}$$

where $\mathbf{F}_L \in \mathbb{C}^{N \times L}$ can be constituted by taking the first L columns of the N-point DFT matrix $\mathbf{F}$ in (5). From (8) and (9) entire MIMO channel frequency response $\mathbf{H} \in \mathbb{C}^{M}$, where $M \equiv N_T N_R N$, can be expressed as below

$$\mathbf{H} = \left[\mathbf{H}^{(1)T}, \mathbf{H}^{(2)T}, ..., \mathbf{H}^{(N_R)T}\right]^T . \tag{10}$$

In the above expression, it is assumed that the whole CFR is spatially uncorrelated. In order to drive an expression of the spatially correlated channel frequency response, $\mathbf{H}_S \in \mathbb{C}^{M}$ in terms of $\mathbf{H}$; we have to define the spatial correlation matrix $\mathbf{R} \in \mathbb{C}^{N_R N_T \times N_R N_T}$ as below [7]

$$\mathbf{R} = \mathbf{R}_{TX} \otimes \mathbf{R}_{RX} \ . \tag{11}$$

Above, $\mathbf{R}_{TX} \in \mathbb{C}^{N_T \times N_T}$ and $\mathbf{R}_{RX} \in \mathbb{C}^{N_R \times N_R}$ are the normalized spatial correlation matrices of the transmit and the receive antennas respectively. From (10) and (11) the spatially correlated channel frequency response can be denoted as

$$\mathbf{H}_S = \sqrt{\mathbf{R}} \otimes \mathbf{H} \ . \tag{12}$$

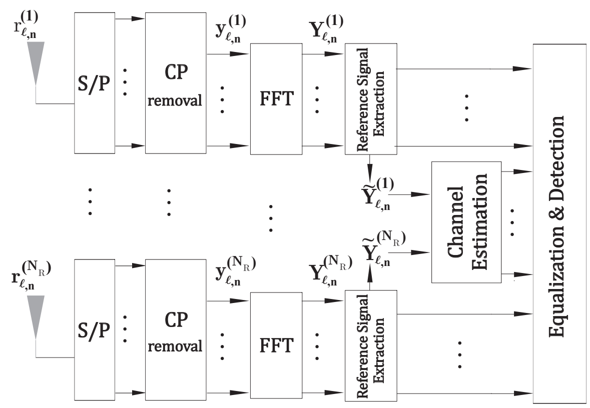

Fig. 2. MIMO-OFDM Receiver scheme for LTE Downlink

Denoting

$$\mathbf{Y} = [\mathbf{Y}_1^T, \mathbf{Y}_2^T, ..., \mathbf{Y}_{N_R}^T]^T \tag{13}$$

as the entire received signal vector $\mathbf{Y} \in \mathbb{C}^{N_R N}$ the whole signal model can be written as in [5]:

$$\mathbf{Y} = (\mathbf{I}_{N_R} \otimes \mathscr{X})\mathbf{H}_S + \mathbf{W} \ . \tag{14}$$

where $\mathbf{W} \in \mathbb{C}^{N_R N}$ is the zero mean white gaussian noise with a covariance matrix of $\mathbf{C}_{\mathbf{W}} = E[\mathbf{W}\mathbf{W}^H] = \sigma^2 \mathbf{I}_{N_R N}$.

III. Channel Estimation

In this section, LS channel estimation and MMSE estimation of the Karhunen-Loéve expansion coefficients will be derived. Assume that only the symbols which contain the reference signal are selected. In the frequency domain signal representation, there exist N_{rs} reference signals. Denoting

$$\tilde{\mathbf{Y}} = (\mathbf{I}_{N_R} \otimes \tilde{\mathscr{X}})\tilde{\mathbf{H}}_S + \tilde{\mathbf{W}} \ , \tag{15}$$

as the received signal vector at the reference signal positions where $\tilde{\mathbf{Y}} \in \mathbb{C}^{N_p}$ and $N_p = N_T N_R N_{rs}$ is the total number of reference signal in the MIMO scheme. In (15) $\tilde{\mathscr{X}}$ can be expressed as

$$\tilde{\mathscr{X}} = [\tilde{\mathbf{X}}^{(1)}, \tilde{\mathbf{X}}^{(2)}, ..., \tilde{\mathbf{X}}^{(N_T)}] \in \Phi^{N_T K_p \times N_T K_p}$$

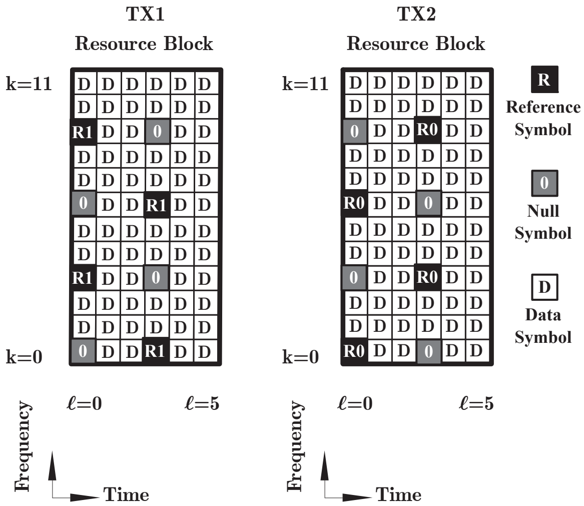

Fig. 3. 3GPP-LTE MIMO scheme downlink signal pattern

A. Least Squares Estimator

The LS estimator of the reference signals can be derived as

$$\tilde{\mathbf{H}}_S = (\mathbf{\Theta}^H \mathbf{\Theta})^{-1} \mathbf{\Theta}^H \tilde{\mathbf{Y}} \ , \tag{16}$$

where $\mathbf{\Theta} \in \mathbb{C}^{\ \mathbf{N_P} \times \mathbf{N_P}}$ can be obtained as $\mathbf{\Theta} = \mathbf{I_{N_R}} \otimes \mathscr{X}$. In LTE MIMO structure, the reference signals are orthogonal to each other. In Figure 3. a simple reference signal orthogonality is depicted. Thus $(\mathbf{\Theta}^H \mathbf{\Theta})^{-1}$ in (16) can be easily derived as in [6] below

$$\tilde{\mathbf{H}}_S = \mathbf{\Theta}^H \tilde{\mathbf{Y}} \ . \tag{17}$$

B. Karhunen-Loéve Expansion

The frequency response of the MIMO channel at reference signal locations $\tilde{\mathbf{H}}_S$, is a zero-mean random variable with covariance matrix $\mathbf{C_H}$. KL transformation makes the channel vector orthogonal such that it can be represented by KL coefficients basis vectors as below

$$\tilde{\mathbf{H}}_S = \sum_{l=1}^{N_p} g_l \psi_l = \mathbf{\Psi} \mathbf{g} \ , \tag{18}$$

where ψ_i's are orthonormal basis vectors constitute $\mathbf{\Psi} = \left[\psi_1, \psi_2, \cdots, \psi_{N_p}\right]$ and g_l's are the KL expansion coefficients defined in vector $\mathbf{g} = \left[g_1, g_2, \cdots, g_{N_p}\right]^T$. Consequently defining $E[\mathbf{g}\mathbf{g}^H] = \mathbf{\Lambda_g}$; the channel covariance matrix at reference signal positions can be easily expressed as

$$\begin{aligned} \mathbf{C_H} &= E[\tilde{\mathbf{H}}_S (\tilde{\mathbf{H}}_S)^H] && (19) \\ &= \mathbf{\Psi} \mathbf{\Lambda_g} \mathbf{\Psi}^H \ . && (20) \end{aligned}$$

In the above equation, if the $\mathbf{\Lambda_g}$ matrix is diagonal, $\mathbf{\Psi} \mathbf{\Lambda_g} \mathbf{\Psi}^H$ expression becomes the Singular Value Decomposition of the $\mathbf{C_H}$ matrix. Thus we can express (15) in a different form

$$\tilde{\mathbf{Y}} = \mathbf{\Theta} \mathbf{\Psi} \mathbf{g} + \tilde{\mathbf{W}} \ . \tag{21}$$

Finally, the MMSE estimator of the KL expansion coefficients can be expressed as in [5]

$$\begin{aligned} \hat{\mathbf{g}} &= \mathbf{\Lambda_g} \left(\mathbf{\Lambda_g} + \sigma^2 \mathbf{I}_{N_p}\right)^{-1} \mathbf{\Psi}^H \mathbf{\Theta}^H \tilde{\mathbf{Y}} \\ &= \mathbf{\Gamma} \mathbf{\Psi}^H \mathbf{\Theta}^H \tilde{\mathbf{Y}} \ . && (22) \end{aligned}$$

$\mathbf{\Gamma}$ can be denoted as

$$\begin{aligned} \mathbf{\Gamma} &= \mathbf{\Lambda_g} \left(\mathbf{\Lambda_g} + \sigma^2 \mathbf{I}_{N_p}\right)^{-1} \\ &= diag\{\frac{\lambda_{g_1}}{\lambda_{g_1} + \sigma^2}, \ldots, \frac{\lambda_{g_{N_p}}}{\lambda_{g_{N_p}} + \sigma^2}\} \ , && (23) \end{aligned}$$

where $\lambda_{g_1}, \lambda_{g_2}, \cdots, \lambda_{g_{N_p}}$'s as the singular values of the $\mathbf{\Lambda_g}$. Assuming the rank of the matrix $\mathbf{\Lambda_g}$ as , the MMSE estimator of the optimum truncated KL expansion can be defined as

$$\mathbf{\Gamma}_{tr} = diag\{\frac{\lambda_{g_1}}{\lambda_{g_1} + \sigma^2}, \ldots, \frac{\lambda_{g_r}}{\lambda_{g_r} + \sigma^2}, 0, \ldots, 0\} \ . \tag{24}$$

As a result, the MMSE estimator of the KL expansion coefficient requires only the division operations of the coefficients instead of huge matrix multiplications.

IV. Simulation

Full channel impulse response is extracted from the one-dimensional linear interpolation of the reference signal at the pilot points. In [2], LTE MIMO Channel parameters are defined for the simulations. In Table I. LTE downlink air interface specifications are defined for different bandwidths. A Bandwidth of 3 MHz is chosen in the simulations. This choice means that working with a number of $N_{RB}^{DL} = 15$ resource blocks. From I, DFT size and the number of occupied subcarriers are defined as $N = 256$, $N_{BW} = 180$ respectively. It is obvious that the total number of the guard bands is parameterized as $N_{GB} = 76$. Modulation type chosen as BPSK. In order to generate the reference signal, L-31 Gold Sequence Pseudo Random Number array is used as depicted in [1]. 2x2 MIMO channel type is chosen. Equalization is performed by LS estimated and interpolated reference signals. A number of r coefficient is computed by the optimum truncated KL expansion coefficient estimator. Reduced rank truncated KL estimator finds $r-1$ coefficients. The transmit and receive antenna's correlation coefficients are defined as $\alpha = 0.3$ and $\beta = 0.3$ respectively. The transmit antenna correlation matrix $\mathbf{R}_{TX}$ and the receive antenna correlation matrix $\mathbf{R}_{RX}$ are defined as

$$\mathbf{R}_{TX} = \begin{bmatrix} 1 & \alpha \\ \alpha & 1 \end{bmatrix}$$

$$\mathbf{R}_{RX} = \begin{bmatrix} 1 & \beta \\ \beta & 1 \end{bmatrix}$$

In Figure 4; the performances of the LS estimator, optimal rank and reduced rank truncated KL expansion MMSE estimators are compared in Bit Error Rate (BER) sense. There exists an error floor for the reduced rank KL MMSE estimator greater than the values of a 20 dB Eb/N0. In Figure 5; BER results are examined according to different correlation coefficients for the same LTE spatial channel model [7].

V. Conclusion

The KL expansion MMSE estimator exhibits a better performance than the LS estimator in the view of BER criteria. Reduced rank truncated KL expansion coefficient estimator performance is also better than the LS at low Eb/N0 values. However at high Eb/N0 values LS estimator exhibits a higher performance than the truncated KL expansion estimator. In addition to increased performance, KL expansion MMSE estimator is also a computationally efficient structure for the LTE downlink MIMO-OFDM systems.

VI. Acknowledgment

This work is supported by The Scientific and Technological Research Council of Turkey (TUBITAK) under grant no. 108E054.

Channel Bandwidth	1.4 MHz	3 MHz	5 MHz	10 MHz	15 MHz	20 MHz
Number of Resource Blocks N_{RB}	6	15	25	50	75	100
Number of used subcarriers	72	180	300	600	900	1200
DFT Size	128	256	512	1024	1536	2048

TABLE I
3GPP-LTE RESOURCE CONFIGURATION [1]

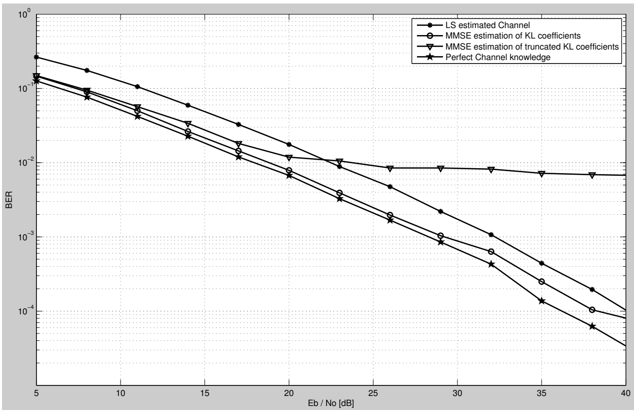

Fig. 4. BER results for estimated and Perfect channel state informations

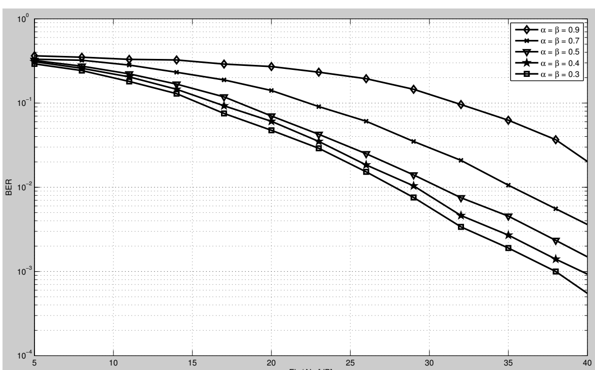

Fig. 5. BER curves for the LTE 2x2 MIMO-OFDM system with different correlation coefficients

REFERENCES

[1] "3GPP TS 36.211 V9.0.0 Evolved Universal Terrestrial Radio Access (E-UTRA); Physical Channels and Modulation (Release 9), Technical report, 3GPP, December 2009 ," 2009.

[2] "3GPP TR 25.996 V9.0.0 Spatial Channel Model for Multiple Input Multiple Output (MIMO) simulations (Release 9), Technical report, 3GPP, December 2009," 2009.

[3] Seongwook Song and A. Singer, "Pilot-Aided OFDM Channel Estimation in the Presence of the Guard Band," Communications, IEEE Transactions on, vol. 55, 2007, pp. 1459-1465.

[4] M. Stege, P. Zillmann, and G. Fettweis, "MIMO channel estimation with dimension reduction," Fifth Symposium on Wireless Personal Multimedia Communication (WPMC), 2002.

[5] B. Karakaya, H. Cirpan, and E. Panayirci, "Channel estimation for MIMO-OFDM systems in fixed broadband wireless applications," Signal Processing and Its Applications, 2007. ISSPA 2007. 9th International Symposium on, 2007, pp. 1-4.

[6] O. Cetin, B. Karakaya, and H. A. Cirpan, "Channel Estimation for 3GPP LTE MIMO-OFDMA systems," in Signal Processing and Communications Applications Conference (SIU), 2010 IEEE 18th, pp. 129-132, 2010.

[7] "Correlation-Based Spatial Channel Modeling," [Online]. Available: http://spcprev.spirentcom.com/documents/5204.pdf